Universiteit
Leiden
The Netherlands

Preclinical and 'near-patient' models for the evaluation of experimental therapy in prostate and bladder cancer

Merbel, A.F. van de

Citation

Merbel, A. F. van de. (2023, September 28). *Preclinical and 'near-patient' models for the evaluation of experimental therapy in prostate and bladder cancer*. Retrieved from https://hdl.handle.net/1887/3642440

Version:	Publisher's Version
License:	Licence agreement concerning inclusion of doctoral thesis in the Institutional Repository of the University of Leiden
Downloaded from:	https://hdl.handle.net/1887/3642440

Note: To cite this publication please use the final published version (if applicable).

5 Anti-Neoplastic Effects of the Antipsychotic Drug Penfluridol in Preclinical Prostate Cancer Models

Arjanneke F. van de Merbel
Maaike H. van der Mark
Tilly Aalders
Niven Mehra
Jack A. Schalken
Geertje van der Horst
Gabri van der Pluijm

Manuscript in preparation

Abstract

The development of castration-resistant prostate cancer (CRPC) and the formation of distant metastases represent clinical unmet needs for prostate cancer patients with advanced disease. The use of drugs for other indications, i.e. drug repurposing, shows great promise for cancer treatment. Drug repurposing could allow new cancer treatments to be introduced relatively quickly and at lower costs. Penfluridol, an approved antipsychotic drug, shows strong cytolytic effects in multiple cancers.

In this study, we have investigated the potential anti-tumor effects of penfluridol in preclinical 'near-patient' prostate cancer models. Penfluridol significantly reduced the viability of monolayer cultures of human prostate cancer cells *in vitro.* Furthermore, penfluridol decreased the viability of three-dimensional cultures and induced cytotoxic effects in *ex vivo* cultured prostate cancer tissue slices from patient-derived xenograft models and freshly isolated prostate cancer biopsies. In conclusion, penfluridol displayed cytotoxic effects in multiple preclinical prostate cancer models. Further research is warranted to address the translational value of our findings.

Introduction

Prostate cancer is the second most common cancer type in men in the Western world (1). The development of castration-resistant prostate cancer (CRPC) and the formation of metastatic disease represent major clinical unmet needs in the treatment of prostate cancer. Therefore, novel treatments for prostate cancer are urgently needed. Epidemiological studies have revealed a reduced incidence of different cancer types, including prostate cancer, in schizophrenic patients (2-4). This suggests that the use of antipsychotics could be protective against the development of cancer. These findings were subsequently further reinforced by several meta-analyses (5, 6). Penfluridol is a long-acting oral antipsychotic drug and is prescribed to treat chronic schizophrenia and other psychiatric disorders (7-10). Interestingly, multiple preclinical studies have demonstrated that penfluridol exerts cytotoxic effects in bladder, breast, colon and pancreatic cancer preclinical models (11-14). Previously, a number of mechanisms of action have been proposed that may underly the observed anti-neoplastic effects, including induction of lysosomal cell death (14, 15), disruption of cholesterol homeostasis (11), inhibition of integrin signaling (12, 16), anti-angiogenic actions (17), repression of prolactin signaling (18), induction of autophagy (13, 19) and blocking of non-homologous end joining (20). To date, the effect of penfluridol on human prostate cancer cells remains unclear. In this study, we have investigated the anti-tumor effects of penfluridol in preclinical human prostate cancer models, including monolayers and three-dimensional cell cultures and *ex vivo* cultured prostate cancer tissue slices.

Material and Methods

Two- and three-dimensional cultures

Human prostate cancer cells lines PC-3M-Pro4luc2, DU145 and 22Rv1, C4, C4-2 and C4-2B4 were cultured in monolayers as described in **Supplementary table 1**. Three dimensional cultures were generated from previously established three-dimensional cultures from prostate cancer bone metastases biopsy material (MSK-PCa1) and prostate cancer liver metastasis PDX model (NM60) as previously described (21-23).

Viability assays

1,500 human prostate cancer cells were seeded per well in 150 µl medium in 96-well plates. After 24 hours, the cells were treated with a dose-range of penfluridol (Sigma-Aldrich) or vehicle (ethanol in medium). The medium was refreshed as indicated. After 72 hours, 20 µl of 3-(4,5 dimethylthiazol-2-yl)-5-(3-carboxymethoxyphenyl)-2-(4-sulfophenyl)-2H-tetrazolium (MTT) (Promega) was added to the culture medium and mitochondrial activity was measured after 2 hours (SpectraMax). Three-dimensional cultures MSK-PCa1 and NM60 were treated with a dose-range of penfluridol. After 3 days, the viability of the cultures was determined by performing a Cell Titer Glo assay according to the manufacturer's protocol (Promega). In parallel to the viability assays, histology was executed on three-dimensional cultures by executing H&E and immunofluorescent stainings for cleaved caspase-3, pancytokeratin and PCNA (**Supplementary table 2**) (23).

Clonogenic assays

100 human prostate cancer cells were seeded in 2 ml of medium in a 6-well plate. After 24 hours, the cells were stimulated with penfluridol for 2 hours. Colonies were fixed and stained with 4% paraformaldehyde and crystal violet after 15-20 days. The number of colonies was counted.

Aldefluor assay

PC-3M-Pro4luc2 cells were treated with a dose-range of penfluridol for 2 hours. Subsequently after 48 hours, 10^6 cells were collected for the Aldefluor Assay. The Aldefluor assay was performed by using the ALDEFLUOR Assay Kit (StemCell Technologies) (24). ALDH substrate was added to the collected cells, resulting into intracellular conversion of the substrate by intracellular ALDH into a fluorescent product. The percentage of $ALDH^{high}$ stem/progenitor-like cells was determined by FACS analysis (LSRII, BD Biosciences) (24).

RT-qPCR

0.5 x 10^6 PC-3M-Pro4luc2 cells were seeded in T25 flasks. After 24 hours, the cells were exposed to a dose-range of penfluridol for 2 hours. After 48 and 72 hours, total RNA was isolated by using TRIzol (Invitrogen). cDNA was synthesized by random primers (Promega) and RT-qPCR was performed with GoTaq Mastermix (Promega) according to the manufacturer's protocol. Gene expression was normalized to GAPDH expression. PCR primer sequences are depicted in **Supplementary table 3.**

Lysosomal associated membrane protein 1 (LAMP-1) immunocytochemistry
A total of 60,000 PC-3M-Pro4luc2 cells were seeded in eight-well chamber slides (ThermoFisher Scientific). After 24 hours, the cells were treated with a dose-range of penfluridol for 2 hours. After 2, 24, 48 and 72 hours, LAMP-1 was visualized by immunofluorescence and confocal microscopy (Leica SP8).

Ex vivo tissue slice culture and scoring
Prostate cancer tumor tissue was obtained from cell line-derived xenografts (CDX) and previously established patient-derived xenograft (PDX) models (23). In addition, primary prostate tumor material was obtained by transurethral resection of the prostate (TURP) after informed consent (Pronet p05.85 and RBUT-ID-PROSTAAT-151). For additional (clinical) details, see **Supplementary table 4**. Prostate cancer tumor tissue was sliced and cultured as previously described (25). After one day of *ex vivo* culture, the prostate cancer tissue slices were treated with 100 µM penfluridol. After exposure to penfluridol for 3 days, the prostate cancer tissue slices were fixed, embedded in paraffin and sectioned (14, 25). Paraffin sections were stained with H&E and immunofluorescent stainings for cleaved caspase-3, pancytokeratin and PCNA were performed in parallel (see **Supplementary table 2**). Images were captured by the SP8 confocal (Leica) and Midi Panoramic slide scanner (3D Histech) (14). The effect of penfluridol on the prostate cancer tissue slices was quantified as previously described (14). In brief, sections were scored based on tissue integrity (H&E staining), the presence of fragmented cytokeratin, proliferating cells (PCNA), and apoptosis (cleaved caspase-3). Cumulative scores of four sections were calculated and displayed in heatmaps whereby a higher score indicates a decrease in tumor tissue quality (14).

Statistical analyses
Statistical analyses were executed by using GraphPad Prism 8.0. One-way ANOVA was performed in order to test for statistical differences in the *in vitro* experiments. * $p<0.05$, ** $p<0.01$, *** $p<0.001$ and **** $p<0.0001$.

Results

Viability of prostate cancer cells upon penfluridol treatment in vitro

Treatment of cultured human prostate cancer cells (PC-3M-Pro4luc2, DU145 and 22Rv1) with a dose-range penfluridol for 72 hours significantly reduced the viability in a panel of human prostate cancer cells (**Figure 1A**). Next, we examined the effect of short penfluridol exposure, i.e. 2 hours, on the viability of human prostate cancer cells (**Figure 1B** and **Supplementary figure 1**). After 2 hours incubation with penfluridol, the medium of the cells was refreshed and the viability of the prostate cancer cells was assessed after 72 hours. Under these circumstances, penfluridol significantly reduced the viability of human prostate cancer cells in vitro (**Figure 1B** and **Supplementary figure 1A**). Clonogenic assays revealed a dose-dependent reduction in the clonogenic capacity of PC-3M-Pro4luc2, DU145 and 22Rv1 cells after 2-hour penfluridol treatment (**Figure 1C** and **Supplementary figure 2A**). In line with these findings, the percentage of ALDH^{high} subpopulation of prostate cancer cells was reduced upon treatment with penfluridol (**Figure 1D**). Penfluridol did not induce changes in the expression of prostate cancer stem cell markers av-integrin (*ITGAV*) and a2-integrin (*ITGA2*) (**Supplementary figure 2B**). Therefore, the exact role of penfluridol on the prostate cancer stem cell population remains unclear.

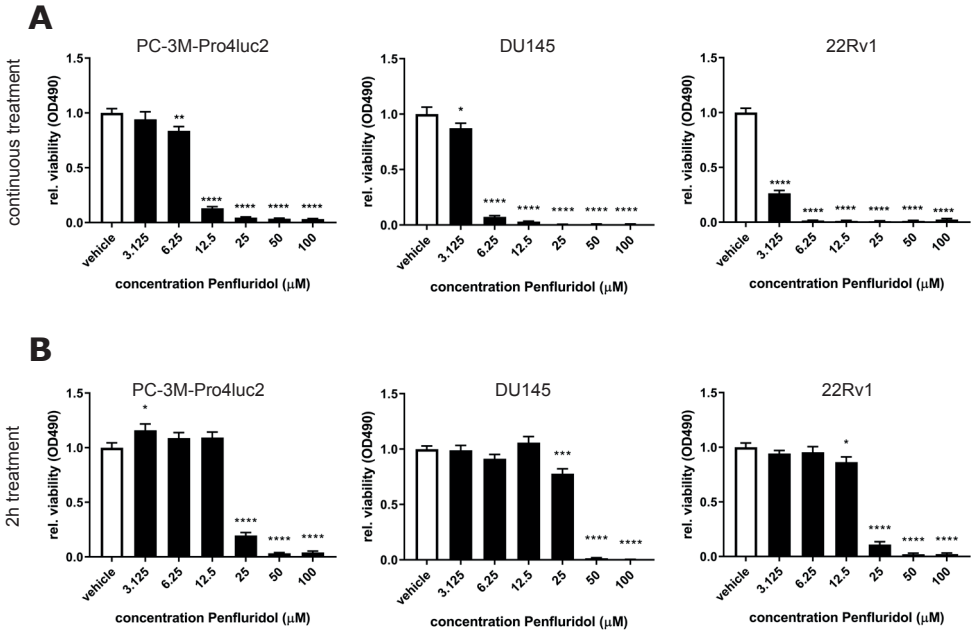

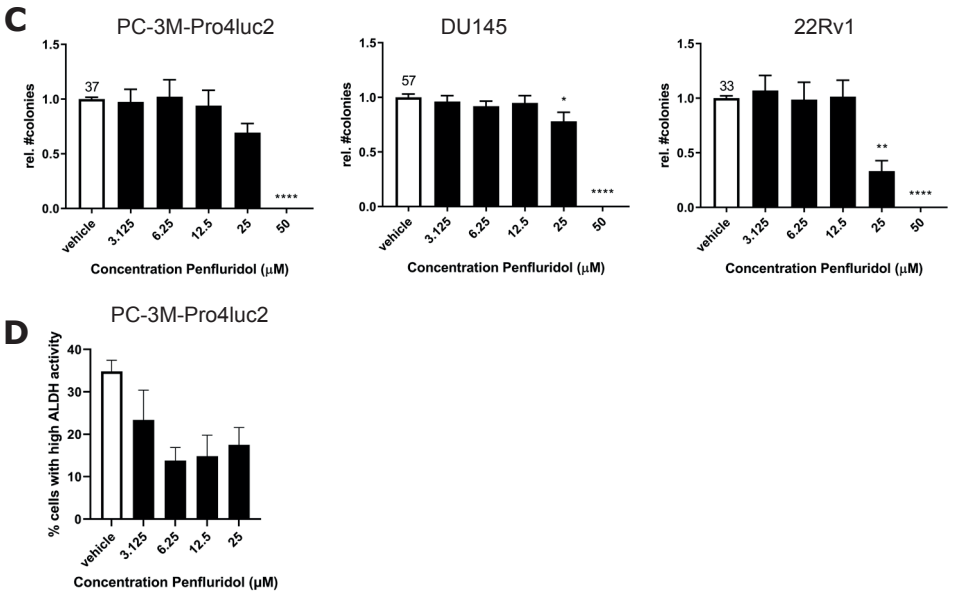

Figure 1 Penfluridol reduces viability and clonogenicity of human prostate cancer monolayer cultures.

*Continuous (**A**) and two-hour (**B**) exposure of human prostate cancer cell lines PC-3M-Pro4luc2, DU145 and 22Rv1 to a dose-range of penfluridol resulted in a reduced viability after 72 hours. Mean +/- standard error of the mean (SEM) (n=3) * p<0.05, ** p<0.01, **** p<0.0001, one-way ANOVA. (**C**) Treatment of human prostate cancer cell lines with penfluridol decreased the number of colonies. Mean +/- standard error of the mean (SEM) (n=3) * p<0.05, ** p<0.01, **** p<0.0001, one-way ANOVA. (**D**) Exposure to penfluridol reduced the percentage of cells with high ALDH activity ($ALDH^{high}$) cells in PC-3M-Pro4luc2 cells. Mean +/- standard error of the mean (SEM) (n=2) * p<0.05, ** p<0.01, **** p<0.0001, one-way ANOVA.*

Next, three-dimensional cultures of MSK-PCa1 cells (prostate cancer bone metastases material (22)) and NM60 cells (prostate cancer liver metastasis PDX model (22, 23)) were treated with a dose-range of penfluridol for 72 hours. Treatment with penfluridol significantly and dose-dependently reduced the viability in three-dimensional cultures of MSK-PCa1 and NM60 prostate cancer cells (**Figure 2A**). Immunohistochemical analyses of MSK-PCa1 confirmed a reduction in proliferation marker PCNA and fragmentation of epithelial marker pan-cytokeratin (panKRT) upon penfluridol exposure. Furthermore, apoptosis was induced (cleaved caspase-3, cCASP-3) and a complete loss of organoid architecture was observed in MSK-PCa1 (**Figure 2B**).

Overall, these results suggest that penfluridol displays anti-tumor effects in monolayers and three-dimensional cultures of human prostate cancer.

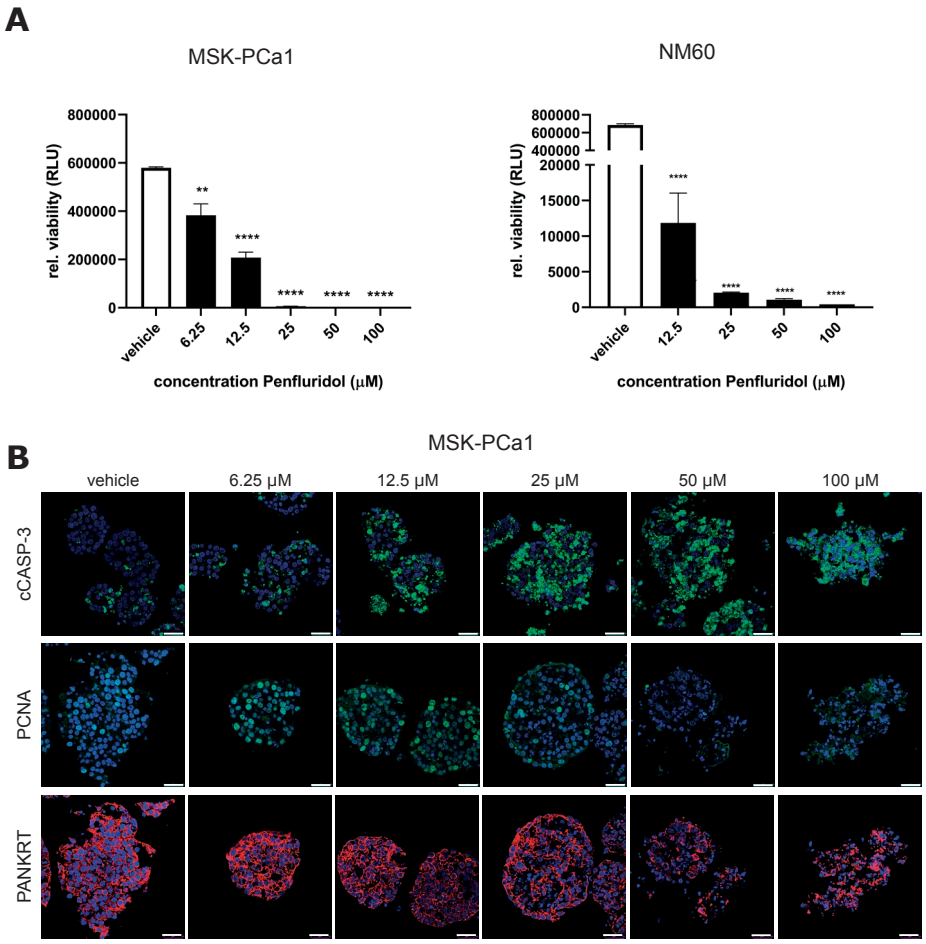

Figure 2 Penfluridoi displays anti-tumor effects in three-dimensional cell cuitures of advanced human prostate cancer.

*Three-dimensional cell cultures bone metastases (MSK-PCa1) and prostate cancer liver metastases (NM60) derived prostate cancer cells were exposed to a dose-range of penfluridol for 72 hours. (**A**) Viability assays revealed a significant dose-dependent decrease in viability after treatment with penfluridol. Mean +/- standard error of the mean (SEM), ** p<0.01, **** p<0.0001, one-way ANOVA (n=3) (**B**) Representative images of three-dimensional MSK-PCa1 cell cultures stained for apoptosis (cleaved caspase-3, cCASP-3 in green), proliferation (proliferating cell nuclear antigen, PCNA in green), epithelial cell marker (pan-cytokeratin PANKRT in red) combined with nuclear staining (DAPI, in blue) indicated decreased cancer cell proliferation and integrity upon penfluridol exposure. Magnification 63x, scale bar = 25 μm*

Penfluridol induces an anti-tumor response in ex vivo cultured prostate cancer tissues

Prostate cancer tissue slices were generated from subcutaneously growing PC-3M-Pro4luc2 tumors and cultured in the presence of 100 µM penfluridol for 3 and 6 days. H&E stainings revealed a lower cell density and the presence of fragmented nuclei in the outer rim of penfluridol-treated tissue slices (red marked areas in **Figure 3A**). Moreover, immunohistochemical analyses indicated a reduction in the number of proliferating cells and an increased presence of apoptotic cells and fragmented cytokeratin upon treatment with penfluridol (**Figure 3B**). The effect of penfluridol was quantified by a scoring system based on loss of tissue architecture, the absence of proliferating cells and the presence apoptotic cells and fragmented cytokeratin (14). Scoring of the tissue slices revealed a slight increase in score after treatment with penfluridol (**Figure 3C**). It should be noted that only tissue in the outer rim of the tissue slices was affected, indicating that, under these experimental circumstances, the distribution of penfluridol was superficial.

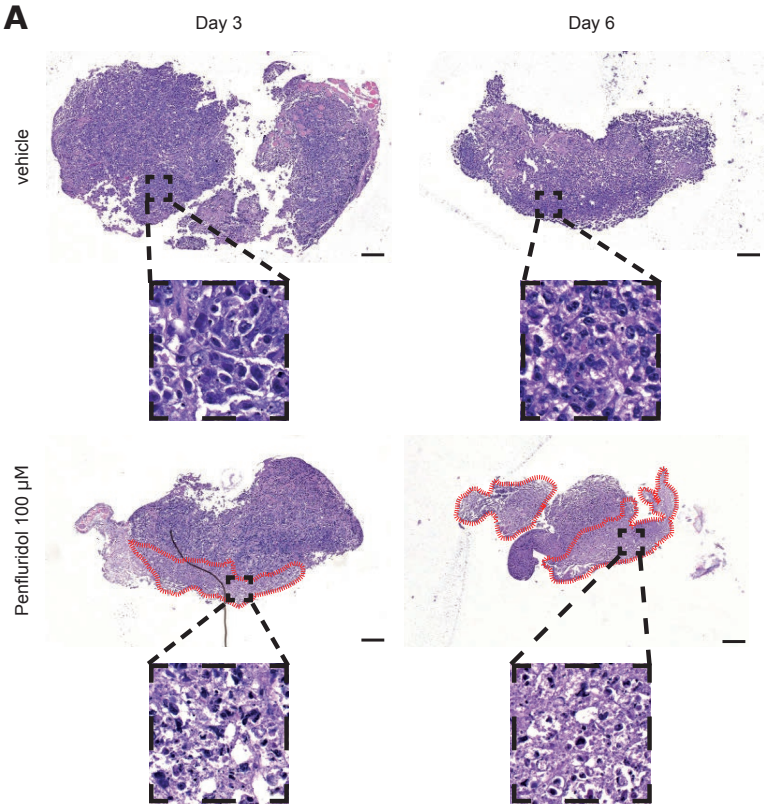

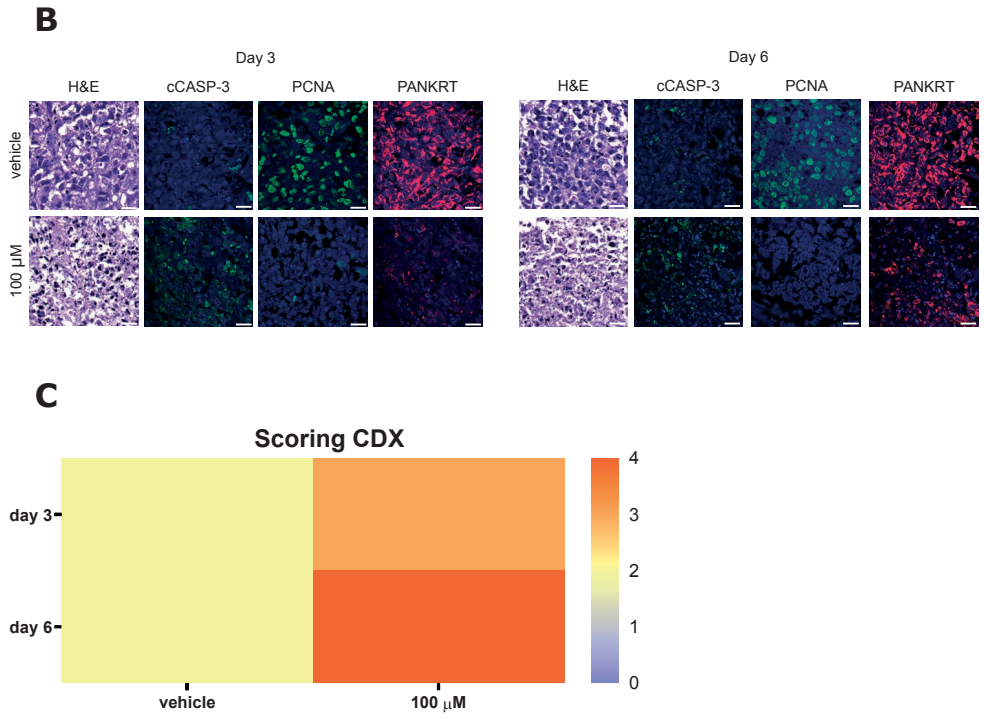

Figure 3 Penfluridol induces cancer cell death in cell line-derived prostate cancer tissue slices. *Prostate cancer tissue slices were generated from a tumor derived from a human prostate cancer cell line derived xenograft (CDX), PC-3M-Pro4luc2, that were subsequently treated in the absence or presence of penfluridol for 3 and 6 days.*

*(**A**) H&E staining revealed a lower tumor cell densities and the presence of fragmented nuclei in the outer rim of penfluridol-treated tissue slices (red marked areas). Magnification 4x, scale bar = 200 µm. (**B**) Representative images of ex vivo cultures tumor tissue slices stained for H&E, apoptosis (cleaved caspase-3, cCASP-3 in green), proliferation (proliferating cell nuclear antigen, PCNA in green), epithelial cell integrity (pan-cytokeratin PANKRT in red) and nuclei (DAPI, in blue) indicated an anti-tumor response after exposure to 100 mM penfluridol. Magnification 63x, scale bar = 25 µm (**C**) PC-3M-Pro4luc2 tissue slices treated with penfluridol were scored based on tissue quality (H&E staining), loss of proliferation (PCNA), induction of apoptosis (cleaved caspase-3) and the presence of fragmented cytokeratin (14). Cumulative scores of four sections were calculated and displayed in heatmaps whereby a higher score indicates a decrease in tissue quality. Scoring of PC-3M-Pro4luc2 tissue slices revealed an increase in cumulative score upon treatment with penfluridol, indicating an overall reduced tissue quality.*

Subsequently, tissue slices were generated from our previously established PDX models PCa-15.01 and NM60 and treated with 100 µM penfluridol for 3 days (**Figure 4A** and **Figure 4B**) (23, 25). Treatment with penfluridol resulted in increased levels of apoptosis, decreased numbers of proliferating tumor cells and loss of tumor cell integrity (**Figure 4A**) leading to an overall increase in tissue score (**Figure 4B**). Hence, these observations indicate that penfluridol displays anti-tumor properties in these ex vivo cultured tumor tissue slices derived from prostate cancer PDX models. Finally, similar anti-tumor effects of penfluridol were found in tissue slices derived from freshly isolated prostate cancer biospies using the same experimental setup (**Figure 4C**). Taken together, these results suggest that penfluridol treatment can induce an anti-tumor response in ex vivo cultured prostate cancer tissue slices.

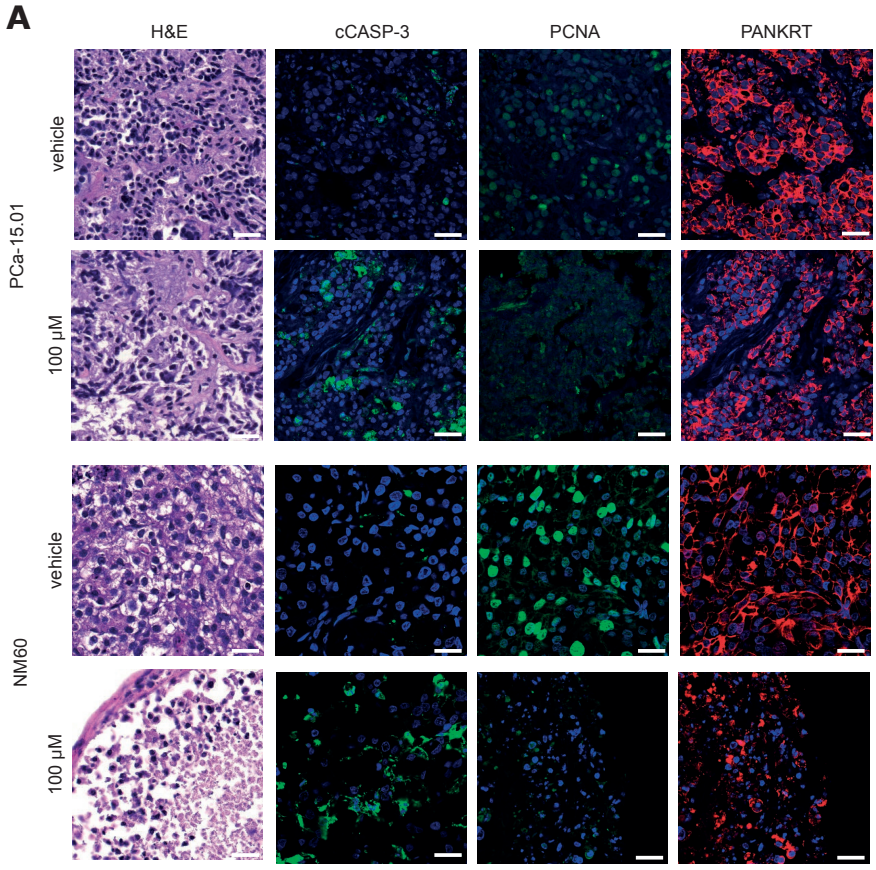

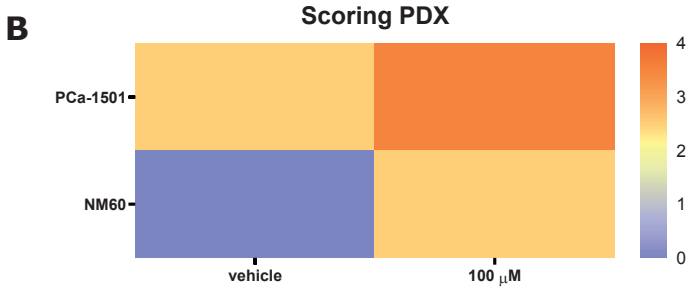
B
Scoring PDX
PCa-1501
NM60
vehicle
100 μM
4
3
2
1
0

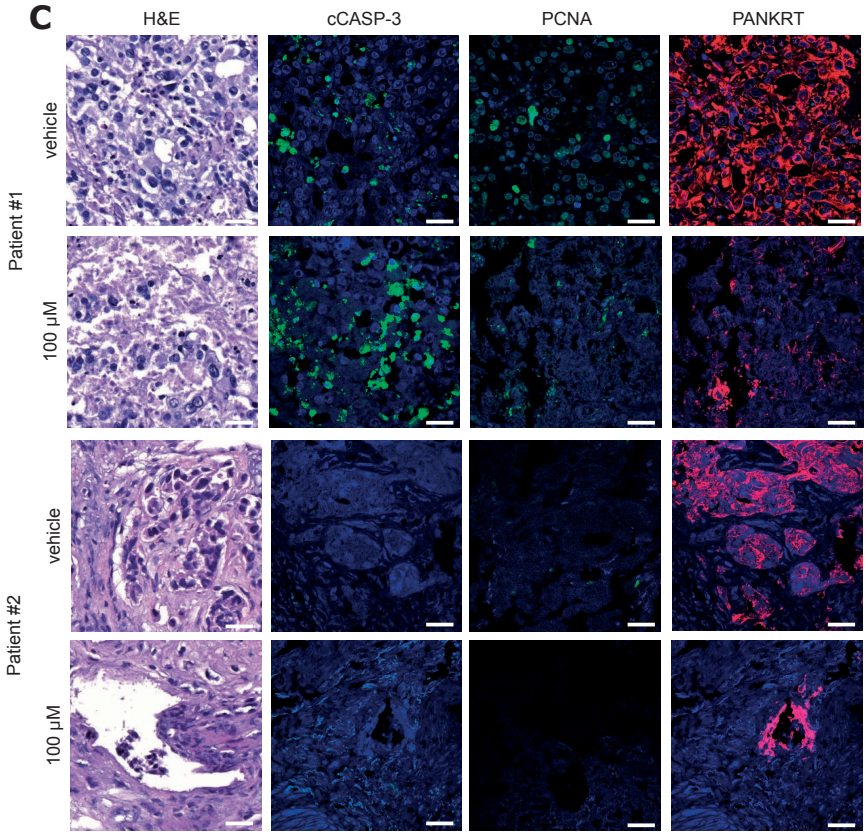
C
H&E
cCASP-3
PCNA
PANKRT
Patient #1
vehicle
100 μM
Patient #2
vehicle
100 μM

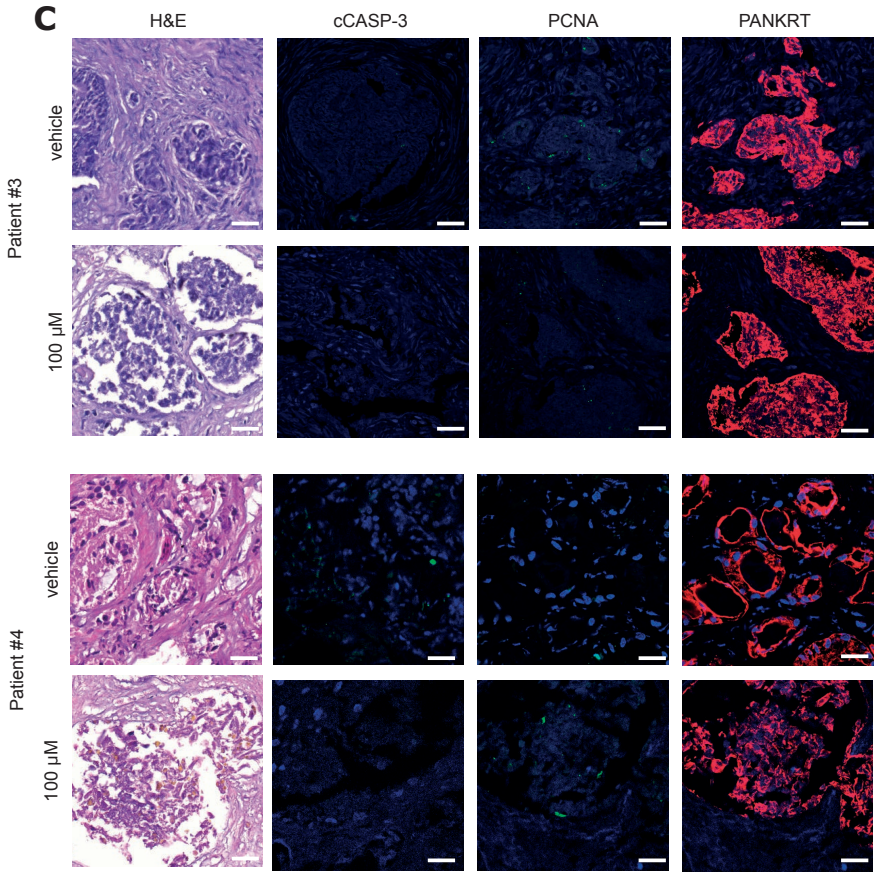

Figure 4 Penfluridol displays anti-tumor effects in *ex vivo* cultured tumor tissue slices from prostate cancer patient-derived xenograft models and primary biopsy samples.

*Tissue slices were generated from patient-derived xenograft (PDX) models PCa-15.01 and NM60 (23) (**A** and **B**) or primary patient biopsies (**C**). Ex vivo treatment of tissue slices resulted in the induction of an anti-tumor response as indicated by histology. Green = PCNA, Red = PANKRT, blue = DAPI. Magnification 63x, scale bar = 25 µm.*

Penfluridol does not affect integrin expression or LAMP-1 distribution in vitro

Previously, several tentative mechanisms of action for penfluridol have been postulated for other tumor types including the induction of lysosomal cell death and modulated integrin expression that may help to explain the anti-tumor effects of penfluridol in prostate cancer cells (12, 14, 16). In order to examine the effect of penfluridol on lysosomal integrity, PC-3M-Pro4luc2 cells were treated with a dose-range of penfluridol for 2 hours.

Immunohistochemical analyses of PC-3M-Pro4luc2 cells with penfluridol for 2 hours revealed no clear changes in lysosome integrity, as assessed by immunocytochemistry for lysosomal-associated membrane protein-1 (LAMP-1) staining after 2, 24, 48 and 72 hours (**Supplementary figure 3A**) (26, 27). Immunocytochemistry did not reveal clear-cut differences in LAMP-1 distribution after treatment with penfluridol. Next, the effect of penfluridol on integrin expression was investigated. PC-3M-Pro4luc2 cells were exposed to a dose-range of penfluridol for 2 hours. After 48 and 72 hours, the expression of multiple integrins was assessed by RT-qPCR. Penfluridol did not induce significant changes in ITGA5, ITGA6, ITGB1 or ITGB4 gene expression after 48 or 72 hours (**Supplementary figure 3B**). These latter observations suggest that other molecular mechanisms may be prevalent in inducing the anti-tumor effects of penfluridol in human prostate cancer cells.

Discussion

In this study, we have identified penfluridol as an anti-tumor agent in human prostate cancer using preclinical, 'near-patient' models (14,23-25). Penfluridol displayed oncolytic effects in multiple preclinical prostate cancer models including monolayer cultures, three-dimensional cultures and ex vivo cultured prostate cancer tissue slices. Our study reports for the first time that penfluridol displays anti-tumor effects in multiple preclinical prostate cancer models.

Penfluridol was discovered in 1968 and was initially developed as an oral antipsychotic drug with a long half-life (7-9). Recently, the class of cationic amphiphilic drugs (CADs), including penfluridol, has drawn substantial attention for displaying anti-neoplastic properties in different tumor types. However, the effects of CADs, including penfluridol, on prostate cancer remained unclear. Multiple mechanistical working mechanisms have been proposed for penfluridol. In this study, no changes in LAMP-1 distribution or integrin gene expression were observed after treatment with penfluridol. Therefore, the working mechanism of penfluridol in human prostate cancer cells remains unknown. Additional future studies are required to dissect the exact working mechanisms of penfluridol in human prostate cancer cells.

Since penfluridol is a clinically-approved agent, the pharmacokinetics, safety and toxicity of penfluridol are well-known (9). Therefore, repurposing of penfluridol for the treatment of prostate cancer might represent a time- and cost-effective approach (28). Clinical studies are warranted to elucidate which subgroup of prostate cancer patients will benefit the most from penfluridol treatment. Our preclinical data suggests that penfluridol is a potent anti-tumor agent in advanced prostate cancer, including CRPC and metastatic prostate cancer. Clinical phase II studies investigating the effect of systemic treatment with penfluridol in advanced prostate cancer patients are needed. The described ex vivo cultures could help in further deciphering which subgroup of patients will benefit most from penfluridol treatment, although further co-clinical studies are warranted to elucidate the predictive value of these cultures. Taken together, in this study we identify penfluridol as a promising anti-cancer agent by inducing cytolytic effects in multiple preclinical human prostate cancer models. We believe that repurposing of penfluridol might represent an interesting option in the treatment of (metastatic) prostate cancer.

Acknowledgments

Authors would like to thank Maria Tsitouridou and Sofi Vassileva for technical assistance.

References

1. Bray F, Ferlay J, Soerjomataram I, Siegel RL, Torre LA, Jemal A. Global cancer statistics 2018: GLOBOCAN estimates of incidence and mortality worldwide for 36 cancers in 185 countries. CA Cancer J Clin. 2018;68(6):394-424.

2. Mortensen PB. The incidence of cancer in schizophrenic patients. J Epidemiol Community Health. 1989;43(1):43-7.

3. Ji J, Sundquist K, Ning Y, Kendler KS, Sundquist J, Chen X. Incidence of cancer in patients with schizophrenia and their first-degree relatives: a population-based study in Sweden. Schizophr Bull. 2013;39(3):527-36.

4. Torrey EF. Prostate cancer and schizophrenia. Urology. 2006;68(6):1280-3.

5. Li H, Li J, Yu X, Zheng H, Sun X, Lu Y, et al. The incidence rate of cancer in patients with schizophrenia: A meta-analysis of cohort studies. Schizophr Res. 2018;195:519-28.

6. Catts VS, Catts SV, O'Toole BI, Frost AD. Cancer incidence in patients with schizophrenia and their first-degree relatives - a meta-analysis. Acta Psychiatr Scand. 2008;117(5):323-36.

7. Balant-Gorgia AE, Balant L. Antipsychotic drugs. Clinical pharmacokinetics of potential candidates for plasma concentration monitoring. Clin Pharmacokinet. 1987;13(2):65-90.

8. Claghorn JL, Mathew RJ, Mirabi M. Penfluridol: a long acting oral antipsychotic drug. J Clin Psychiatry. 1979;40(2):107-9.

9. Migdalof BH, Grindel JM, Heykants JJ, Janssen PA. Penfluridol: a neuroleptic drug designed for long duration of action. Drug Metab Rev. 1979;9(2):281-99.

10. Tuan NM, Lee CH. Penfluridol as a Candidate of Drug Repurposing for Anticancer Agent. Molecules. 2019;24(20).

11. Wu L, Liu YY, Li ZX, Zhao Q, Wang X, Yu Y, et al. Anti-tumor effects of penfluridol through dysregulation of cholesterol homeostasis. Asian Pac J Cancer Prev. 2014;15(1):489-94.

12. Ranjan A, Gupta P, Srivastava SK. Penfluridol: An Antipsychotic Agent Suppresses Metastatic Tumor Growth in Triple-Negative Breast Cancer by Inhibiting Integrin Signaling Axis. Cancer Res. 2016;76(4):877-90.

13. Ranjan A, German N, Mikelis C, Srivenugopal K, Srivastava SK. Penfluridol induces endoplasmic reticulum stress leading to autophagy in pancreatic cancer. Tumour Biol. 2017;39(6):1010428317705517.

14. van der Horst G, van de Merbel AF, Ruigrok E, van der Mark MH, Ploeg E, Appelman L, et al. Cationic amphiphilic drugs as potential anticancer therapy for bladder cancer. Mol Oncol. 2020;14(12):3121-34.

15. Ellegaard AM, Bach P, Jäättelä M. Targeting Cancer Lysosomes with Good Old Cationic Amphiphilic Drugs. Rev Physiol Biochem Pharmacol. 2021.

16. Hedrick E, Li X, Safe S. Penfluridol Represses Integrin Expression in Breast Cancer through Induction of Reactive Oxygen Species and Downregulation of Sp Transcription Factors. Mol Cancer Ther. 2017;16(1):205-16.

17. Srivastava S, Zahra FT, Gupta N, Tullar PE, Srivastava SK, Mikelis CM. Low Dose of Penfluridol Inhibits VEGF-Induced Angiogenesis. Int J Mol Sci. 2020;21(3).

18. Dandawate P, Kaushik G, Ghosh C, Standing D, Ali Sayed AA, Choudhury S, et al. Diphenylbutylpiperidine Antipsychotic Drugs Inhibit Prolactin Receptor Signaling to Reduce Growth of Pancreatic Ductal Adenocarcinoma in Mice. Gastroenterology. 2020;158(5):1433-49.e27.

19. Ranjan A, Srivastava SK. Penfluridol suppresses pancreatic tumor growth by autophagy-mediated apoptosis. Sci Rep. 2016;6:26165.

20. Du J, Shang J, Chen F, Zhang Y, Yin N, Xie T, et al. A CRISPR/Cas9-Based Screening for Non-Homologous End Joining Inhibitors Reveals Ouabain and Penfluridol as Radiosensitizers. Mol Cancer Ther. 2018;17(2):419-31.

21. Drost J, Karthaus WR, Gao D, Driehuis E, Sawyers CL, Chen Y, et al. Organoid culture systems for prostate epithelial and cancer tissue. Nat Protoc. 2016;11(2):347-58.

22. Gao D, Vela I, Sboner A, Iaquinta PJ, Karthaus WR, Gopalan A, et al. Organoid cultures derived from patients with advanced prostate cancer. Cell. 2014;159(1):176-87.

23. van de Merbel AF, van der Horst G, van der Mark MH, Bots STF, van den Wollenberg DJM, de Ridder CMA, et al. Reovirus mutant jin-3 exhibits lytic and immune-stimulatory effects in preclinical human prostate cancer models. Cancer Gene Ther. 2021.

24. van den Hoogen C, van der Horst G, Cheung H, Buijs JT, Lippitt JM, Guzmán-Ramírez N, et al. High aldehyde dehydrogenase activity identifies tumor-initiating and metastasis-initiating cells in human prostate cancer. Cancer Res. 2010;70(12):5163-73.

25. van de Merbel AF, van der Horst G, van der Mark MH, van Uhm JIM, van Gennep EJ, Kloen P, et al. An ex vivo Tissue Culture Model for the Assessment of Individualized Drug Responses in Prostate and Bladder Cancer. Front Oncol. 2018;8:400.

26. Alvarez-Valadez K, Sauvat A, Fohrer-Ting H, Klein C, Kepp O, Kroemer G, et al. A novel tool for detecting lysosomal membrane permeabilization by high-throughput fluorescence microscopy. Methods Cell Biol. 2021;165:1-12.

27. Eskelinen EL. Roles of LAMP-1 and LAMP-2 in lysosome biogenesis and autophagy. Mol Aspects Med. 2006;27(5-6):495-502.

28. Kaushik I, Ramachandran S, Prasad S, Srivastava SK. Drug rechanneling: A novel paradigm for cancer treatment. Semin Cancer Biol. 2020.

Supplementary table 1 Cell culture media for two-dimensional cultures.

Cell line	Medium	Supplements
PC-3M-Pro4luc2 (derived from PC-3M-Pro4 RRID:CVCL_D579)	Dulbecco's Modified Eagle medium (DMEM) (Life technologies, Gibco, 31966-021)	10% FCII (Hyclone), 100 units/ml penicillin, 50 µg/ml streptomycin (Life Technologies) 800 µg/mL of G-418 (Sigma)
DU145 (RRID:CVCL_0105)	RPMI 1640 (Lonza, BE12-167F)	10% FBS, 100 units/ml penicillin, 50 µg/ml streptomycin (Life Technologies), GlutaMAX (Life Technologies)
22Rv1 (RRID:CVCL_1045)	RPMI 1640 (Lonza, BE12-167F)	10% FBS, 100 units/ml penicillin, 50 µg/ml streptomycin, GlutaMAX
C4 (RRID:CVCL_4783)	T medium: Dulbecco's Modified Eagle medium (DMEM) (Life technologies, Gibco, 31966-021) and Ham F-12K (Life Technologies, Gibco 21127-022) 4:1	10% FBS, 5 ml Insulin-transferrin-selenium (Life Technologies), 1 ml Biotin 0.125 mg/ml (Sigma), 1 ml Adenine 12.5 mg/ml (Sigma), 1 ml T3 6.825 ng/ml (Sigma) and 100 units/ml penicillin, 50 µg/ml streptomycin (Life Technologies)

Supplementary table 1 Cell culture media for two-dimensional cultures continued.

Cell line	Medium	Supplements
C4-2 (RRID:CVCL_4782)	T medium: Dulbecco's Modified Eagle medium (DMEM)(Life technologies, Gibco, 31966-021) and Ham F-12K (Life Technologies, Gibco 21127-022) 4:1	10% FBS, 5 ml Insulin-transferrin-selenium (Life Technologies), 1 ml Biotin 0.125 mg/ml (Sigma), 1 ml Adenine 12.5 mg/ml (Sigma), 1 ml T3 6.825 ng/ml (Sigma) and 100 units/ml penicillin, 50 µg/ml streptomycin (Life Technologies)
C4-2B (RRID:CVCL_4784)	T medium: Dulbecco's Modified Eagle medium (DMEM)(Life technologies, Gibco, 31966-021) and Ham F-12K (Life Technologies, Gibco 21127-022) 4:1	10% FBS, 5 ml Insulin-transferrin-selenium (Life Technologies), 1 ml Biotin 0.125 mg/ml (Sigma), 1 ml Adenine 12.5 mg/ml (Sigma), 1 ml T3 6.825 ng/ml (Sigma) and 100 units/ml penicillin, 50 µg/ml streptomycin (Life Technologies)

Supplementary Table 2 Antibodies used for immunofluorescence stainings.

Target	Species	Supplier	Dilution
Pan cytokeratin	Rabbit	Abcam ab217916	1:500
PCNA	Mouse	Sigma Aldrich P8825	1:2000
Cleaved caspase-3	Rabbit	Cell Signaling 9661L	1:500
Anti-mouse Alexa Fluor 488	Donkey	Life Technologies A-21202	1:250
Anti-rabbit Alexa Fluor 488	Donkey	Life Technologies A-21206	1:250
Anti-mouse Alexa Fluor 555	Donkey	Life TechnologiesA-31570	1:250
Anti-rabbit Alexa Fluor 555	Donkey	Life Technologies A-31572	1:250

Supplementary Table 3 Primer sequences for RT-qPCR.

Target	Primer sequence
GAPDH FW	GACAGTCAGCCGCATCTTC
GAPDH RV	GCAACAATATCCACTTTACCAGAG
Alphav-integrin FW	GCTGGACTGTGGAGAAGAC
Alphav-integrin RV	AAGTGAGGTTCAGGGCATTC
Alpha2-integrin FW	TTTGGTAGTGTGCTGTGTTC
Alpha2-integrin RV	GACTCTTCCTTCCTCTTTCTTTAG
Alpha5-integrin FW	AGTCCTCACTGTCCAGCTCA
Alpha5-integrin RV	GCTCAGTGGCTCCTTCTCTG
Alpha6-integrin FW	GTCGGTTATAATCCTTCAATATCAATTGT
Alpha6-integrin RV	TTGGGCTCAGAACCTTGGTTT
Beta1-integrin FW	AGCAACGGACAGARCTGCAA
Beta1-integrin RV	GCTGGGGTAATTTGTCCCGA
Beta4-integrin FW	CTGTGTGCACGAGGGACATT
Beta4-integrin RV	AAGGCTGACTCGGTGGAGAA

Supplementary Table 4 Model and Patient characteristics.

Tumour model / patient number	Source	Treatment history	Clinical status	References
MSK-PCa1	L2 vertebral body	Androgen-deprivation therapy, bicalutamide	mCRPC	(22)
PCa-15.01	Prostatectomy (hormone naïve)	No previous treatment	T3NxM+ Gleason 4+5 PSA>5000 ug/l	(23)
NM60	Needle biopsy liver metastasis (CRPC)	Zoladex, Docetaxel, Abiraterone, radiotherapy, Cabazitaxel, Carboplatin, Olaparib	PSA:81.0 ug/l	(23)
Patient #1	Transurethral resection	EBRT, LHRH agonist, Enzalutamide	T4N+M+ Gleason 4+4 PSA:52.5 ug/l	N.A.

Supplementary Table 4 Model and Patient characteristics Continued.

Tumour model / patient number	**Source**	**Treatment history**	**Clinical status**	**References**
Patient #2	Transurethral resection	LHRH agonist	T3bNxMx Gleason 3+4 PSA:7.5 ug/l	N.A.
Patient #3	Transurethral resection	Androgen deprivation	T3bN0Mx Gleason 4+4 PSA:15.0 ug/l	N.A.
Patient #4	Transurethral resection	EBRT, Bicalutamide, Goserelin	T3aN0M0 Gleason 4+5 PSA:14.23 ug/l	N.A.

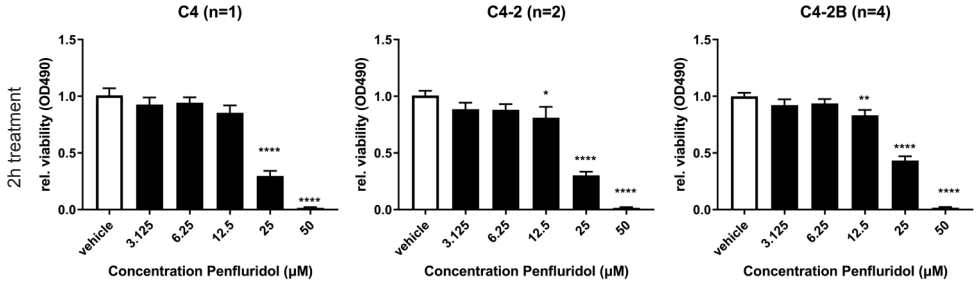

Supplementary figure 1 A 2-hour exposure of penfluridol induces a reduction in viability in C4, C4-2 and C4-2B4 cells.

*Human prostate cancer cell lines C4, C4-2 and C4-2B4 were exposed to a dose-range of penfluridol for 2 hours and subsequently the viability was assessed after 72 hours. Penfluridol induced a dose-dependent and significant reduction in viability in C4, C4-2 and C4-2B4 cells. Mean +/- standard error of the mean (SEM) * p<0.05, ** p<0.01, **** p<0.0001, one-way ANOVA. (Number of independent replicates is stated in the figure).*

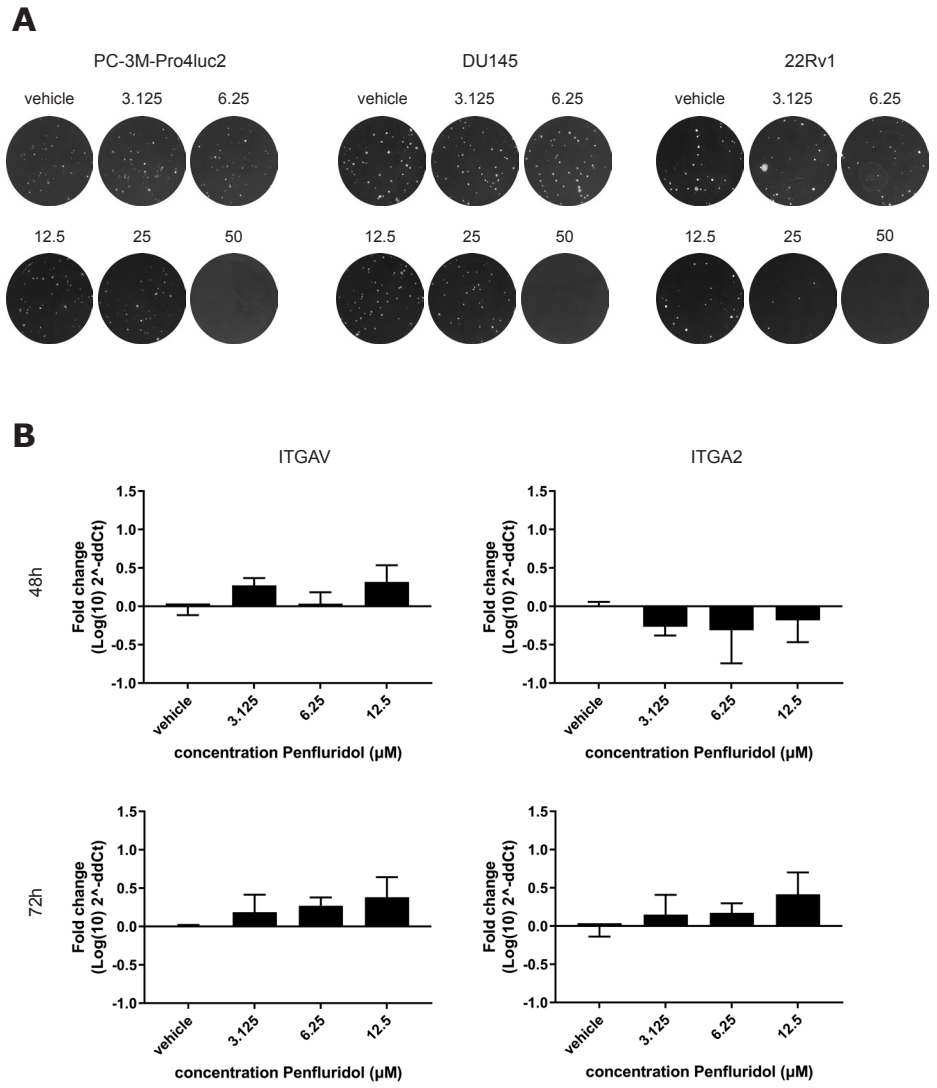

Supplementary figure 2 The effect of penfluridol on clonogenicity and prostate cancer stem cell markers.

*(**A**) Representative images of colonies PC-3M-Pro4luc2, DU145 and 22Rv1 cells after treatment with penfluridol quantified in figure 1. (**B**) No significant changes were observed in mRNA levels of av-integrin and a2-integrin after exposure to penfluridol. Log_{10} change +/- standard error of the mean (SEM) (n=2).*

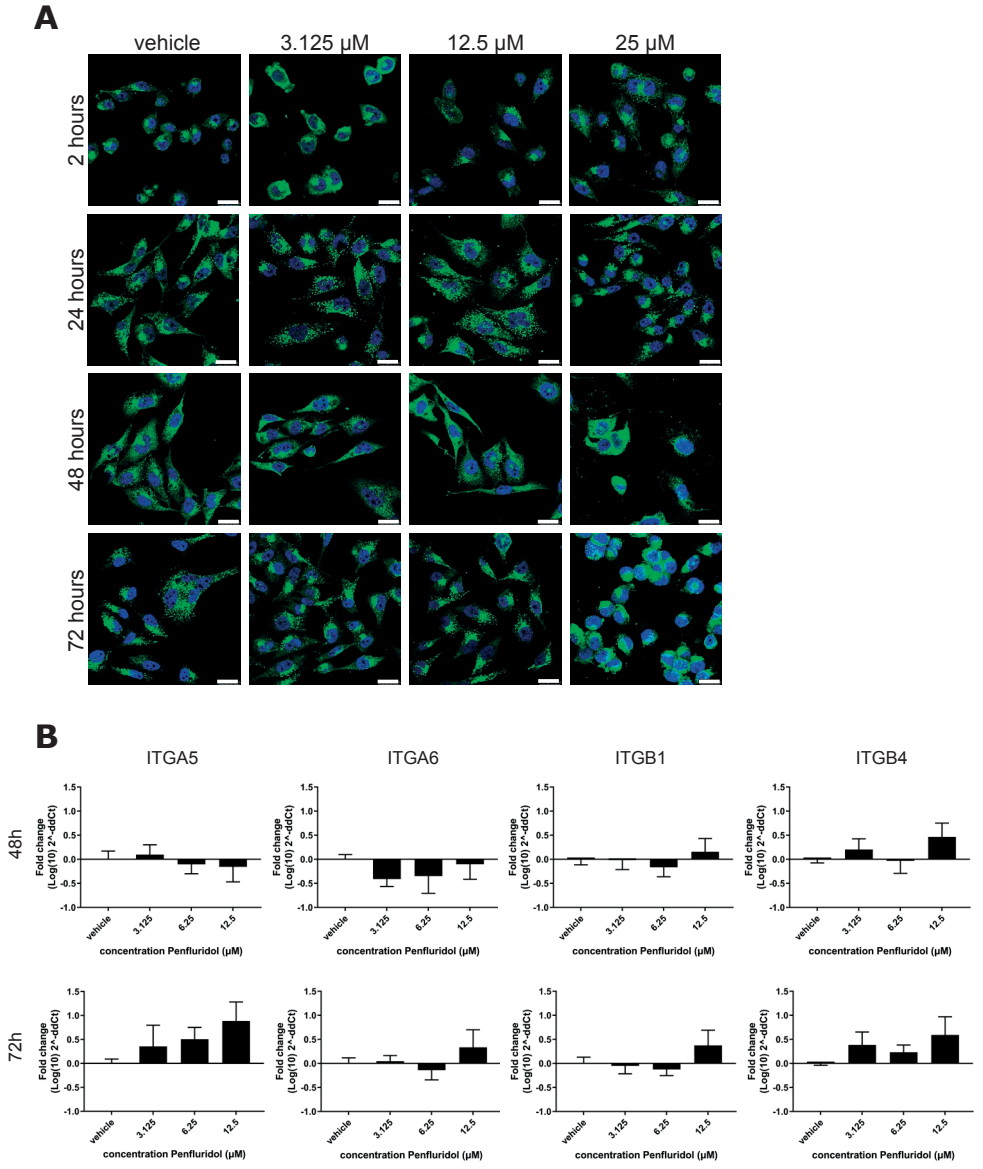

Supplementary figure 3 Penfluridol does not affect LAMP-1 distribution or integrin mRNA expression in PC-3M-Pro4luc2 cells *in vitro.*

*(**A**) Lysosomal membrane-associated protein-1 (LAMP-1, green) distribution in PC-3M-Pro4luc2 cells (DAPI, nuclei = blue) remained unaffected after treatment with penfluridol. Magnification 63x, scale bar = 25 µm. (**B**) Penfluridol did not alter mRNA expression of ITGA5, ITGA6, ITGB1 and ITGB4 in PC-3M-Pro4luc2 cells. Log_{10} change +/- standard error of the mean (SEM) (n=2).*